



## Original article

# Purification and characterization of anti-tubercular and anticancer protein from *Staphylococcus hominis* strain MANF2: *In silico* structural and functional insight of peptide

Ameer Khusro<sup>a</sup>, Chirom Aarti<sup>a</sup>, B. Mahizhaveni<sup>b</sup>, Azger Dusthacker<sup>b</sup>, Paul Agastian<sup>a,\*</sup>, Galal Ali Esmail<sup>c</sup>, Abdul-Kareem Mohammed Ghilan<sup>c</sup>, Naif Abdullah Al-Dhabi<sup>c</sup>, Mariadhas Valan Arasu<sup>c,\*</sup>

<sup>a</sup> Research Department of Plant Biology and Biotechnology, Loyola College (Autonomous), University of Madras, Chennai 34, Tamil Nadu, India

<sup>b</sup> Department of Bacteriology, National Institute for Research in Tuberculosis, ICMR, Sathyamoorthy Road, Chetpet, Chennai 31, Tamil Nadu, India

<sup>c</sup> Department of Botany and Microbiology, College of Science, King Saud University, P.O. Box 2455, Riyadh 11451, Saudi Arabia



## ARTICLE INFO

## Article history:

Received 17 December 2019

Revised 7 January 2020

Accepted 16 January 2020

Available online 27 January 2020

## Keywords:

Anti-tubercular

Anticancer

*In silico* tools

MALDI-TOF MS/MS

Protein

*Staphylococcus hominis*

## ABSTRACT

The present context was investigated to purify and characterize anti-tubercular as well as anticancer protein from fermented food associated *Staphylococcus hominis* strain MANF2. Initially, the anti-tubercular potency of strain MANF2 was assessed against *Mycobacterium tuberculosis* H37Rv using luciferase reporter phase assay which revealed pronounced relative light unit (RLU) reduction of  $92.5 \pm 1.2\%$ . The anticancer property of strain MANF2 was demonstrated against lung cancer (A549) and colon cancer (HT-29) cell lines using MTT assay which showed reduced viabilities. Anti-tubercular activities of the purified protein were observed to be increased significantly ( $P < 0.05$ ) ranging from  $34.6 \pm 0.3$  to  $71.4 \pm 0.4\%$  of RLU reduction. Likewise, the purified protein showed significantly ( $P < 0.05$ ) reduced viabilities of A549 and HT-29 cancer cells with  $IC_{50}$  values of 46.6 and 48.9  $\mu\text{g}/\text{mL}$ , respectively. The nominal mass of the purified protein was found to be 7712.3 Da as obtained from MALDI-TOF MS/MS spectrum. The protein showed the sequence homology with 1–336 amino acids of Glyceraldehyde-3-phosphate dehydrogenase from *Staphylococcus* sp., thus, categorizing as a new class of Glyceraldehyde-3-phosphate dehydrogenase-like protein. The amino acid sequence of the most abundant peptide ( $m/z = 1922.12$ ) in the purified protein was obtained as 'KAIGLVIPEIDGKLDGGAQRV' and it was identified as peptide NMANF2. *In silico* tools predicted significant stereo-chemical, physiochemical, and functional characteristics of peptide NMANF2. In a nutshell, protein purified from strain MANF2 can certainly be used as an ideal therapeutic agent against tuberculosis and cancer (lung and colon).

© 2020 The Author(s). Published by Elsevier B.V. on behalf of King Saud University. This is an open access article under the CC BY-NC-ND license (<http://creativecommons.org/licenses/by-nc-nd/4.0/>).

## 1. Introduction

Over the past few decades, Tuberculosis (TB) remains one of the deadliest neglected infectious diseases causing millions of mortalities globally (Al-Dhabi et al., 2016, 2019). Despite the discovery of first-line and second-line anti-tubercular drugs, TB therapy has become challenging due to the emergence of drug-resistant strains

of *Mycobacterium tuberculosis*. Additionally, the complex and time-consuming therapeutic regimens (6–9 months) as well as co-infection with human immunodeficiency virus (HIV) make the treatment process expensive and disputing for the patients. As per the recent report of World Health Organization (WHO), approximately 10.4 million people were found to be infected with TB globally, 10% of which were co-infected with HIV (Khusro et al., 2016). Surprisingly, the medical system lacks the approval of any new anti-tubercular drugs in the past 40 years (Al-Dhabi et al., 2019a, 2019b). Thus, the dream of End-TB strategy is turning bleak which is irrefutably accentuating worldwide researchers to investigate propitiously for TB therapeutics in future.

Lung cancer or lung carcinoma is characterized by uncontrolled cell growth in the lung tissues. It is the most common cause of cancer-related deaths in men and second most common in women after breast cancer (Al-Dhabi et al., 2019; Al-Dhabi et al.,

\* Corresponding authors.

E-mail addresses: [agastian@loyolacollege.edu](mailto:agastian@loyolacollege.edu) (P. Agastian), [mvalanarasu@ksu.edu.sa](mailto:mvalanarasu@ksu.edu.sa) (M.V. Arasu).

Peer review under responsibility of King Saud University.



Production and hosting by Elsevier

<https://doi.org/10.1016/j.sjbs.2020.01.017>

1319-562X/© 2020 The Author(s). Published by Elsevier B.V. on behalf of King Saud University.

This is an open access article under the CC BY-NC-ND license (<http://creativecommons.org/licenses/by-nc-nd/4.0/>).

2019d; World Cancer Report, 2014). Considering the uncontrolled global burden of TB and cancer (lung cancer and colon cancer), there is desperate indispensability to identify quintessential therapeutic agents from un/less exploited sources with conspicuous activities.

Bacteria associated antimicrobial proteins or peptides manifest growth inhibitory attributes against diversified groups of pathogens (Al-Dhabi et al., 2019, 2020). These ribosomally synthesized bioactive proteins or peptides are produced extensively by gram positive bacteria. Amongst disparate gram positive bacteria, *Staphylococcus* spp. are creating enormous interest which are known to produce distinct classes of antimicrobial proteins or bacteriocins (Al-Dhabi et al., 2018, 2019; Bastos et al., 2009; Al-Dhabi et al., 2018b). Plethora of studies has demonstrated the production, purification, and characterization of staphylococcal proteins (Hale and Hinsdill, 1973; Navartana et al., 1998; Iqbal et al., 2001; Nascimento et al., 2005; Sung et al., 2010). These proteins or peptides showed growth inhibitory activities not only against *Staphylococcus* spp. but also against other microbiota (De-Oliveira et al., 1998). In the past few years, staphylococcal peptides exhibited antagonistic characteristics against *Micrococcus luteus* (Saeed et al., 2004), *Corynebacterium fimi* (Nascimento et al., 2005), *Staphylococcus aureus* (Sung et al., 2010; Kim et al., 2010; Arasu et al., 2013; Wladyka et al., 2015), and *Listeria monocytogenes* (Matikevičienė et al., 2017). In a like manner, proteins from varied group of bacteria have depicted selective toxicity against diverse cancer cells viz. breast cancer, lung cancer, colon cancer, and bone cancer (Kaur and Kaur, 2015; Arasu et al., 2017). In spite of the exemplary anticancer features of gram positive bacteria, the exploitation of *Staphylococcus* sp. associated proteins/peptides as anticancer agents, particularly against lung and colon cancer cell lines is undetermined yet. Considering this, a cogent endeavour was commenced in this context to purify anti-tubercular and anticancer protein from *Staphylococcus hominis*. Further, the structure, physiological, and functional parameters of the most abundant peptide was analyzed through disparate bioinformatics tools.

## 2. Materials and methods

### 2.1. Bacterium of interest

*Staphylococcus hominis* strain MANF2, previously isolated from *Koozh* (a traditional fermented food of Tamil Nadu, India) was used in the present context (Khusro et al., 2018a). Strain MANF2 was sub-cultured at 30 °C for 48 h in 250 mL Erlenmeyer flasks constituting 50 mL of de Man Rogose Sharpe (MRS) broth (HiMedia laboratories) medium for further experiments.

### 2.2. Anti-tubercular property of strain MANF2

The cell free neutralized supernatant (CFNS) of strain MANF2 was used to determine the anti-tubercular activity against *Mycobacterium tuberculosis* H37Rv. The CFNS was obtained by inoculating strain MANF2 into autoclaved MRS medium and incubating for 48 h at 30 °C. The culture was centrifuged at 8000g for 10 min and the supernatant was collected for subjecting it to membrane filtration (0.22 µm). Further, the filtered supernatant was neutralized using 1 N NaOH solution. The anti-tubercular activity of the CFNS of strain MANF2 was assessed as per luciferase reporter phase (LRP) assay (Khusro et al., 2018b).

### 2.3. Anticancer activity of CFNS of strain MANF2

Anticancer activity of the CFNS of strain MANF2 was evaluated against lung cancer cells (A549) and colon cancer cells (HT-29)

using MTT [3-(4,5-dimethylthiazol-2-yl)-2,5-diphenyltetrazolium bromide] assay (Mosmann, 1983). Doxorubicin (Sigma) was used as positive control. The absorbance was read at 620 nm using an ELISA multi-well plate reader according to the equation as given below.

$$\% \text{ viability} = \frac{\text{Absorbance of sample}}{\text{Absorbance of control}} \times 100$$

### 2.4. Purification of protein from strain MANF2

The log phase grown culture was inoculated into autoclaved MRS medium aseptically and incubated at 30 °C for 48 h. The bacterial culture was centrifuged at 8000g for 15 min at 4 °C. The supernatant was collected, neutralized, and precipitated with varied saturation levels (40, 50, 60, 70, and 80%) of ammonium sulphate. The precipitated protein samples were collected after centrifugation at 10,000g for 15 min at 4 °C. The resulting pellets were re-suspended in sodium phosphate buffer (0.1 M, pH 7.0) for the determination of total protein content using Bradford assay (Bradford, 1976). The saturation level showing maximum protein content was further used for dialysis using dialysis membrane (1.0 kDa cut-off). Total protein content of dialysed sample was estimated according to Bradford assay (Bradford, 1976). DEAE-Cellulose column chromatography was used for further purification process. Sample was eluted at the flow rate of 0.5 mL/min. The gradient elution was carried out using 0.2, 0.3, 0.4, and 0.5 M NaCl in the same buffer. Fractions were collected and tested for anti-tubercular activities according to the LRP assay as mentioned in the previous study (Khusro et al., 2018b). Fraction showing maximum anti-tubercular activity was used for determining total protein content (Bradford, 1976). The purity and molecular mass of the most active fraction were determined using Sodium Dodecyl Sulphate-Polyacrylamide Gel Electrophoresis (SDS-PAGE) with 4% stacking gel and 12% separating gel. Protein band was observed and its molecular mass was calculated based on the relative mobility of the standard marker (14.3–66 kDa).

### 2.5. Fourier transform infra-red (FT-IR) spectroscopy

Three milligrams of purified protein were mixed with 300 mg of potassium bromide (FT-IR grade) for the analysis of the functional group as reported by Esther Lydia et al. (2019).

### 2.6. Anti-tubercular activity of purified protein

*M. tuberculosis* H37Rv was grown in the presence of various concentrations (10–50 µg/mL) of purified protein and the anti-tubercular activity was estimated according to the methodology as mentioned in the previous study (Khusro et al., 2018a). Rifampicin was used as positive control.

### 2.7. Characterization of purified protein-

#### 2.7.1. Effect of pH

pH of the purified protein (1 mg/mL) was adjusted from 3.0 to 8.0 using 1 N HCl and 1 N NaOH. Samples were incubated at 37 °C for 3 h and residual anti-tubercular activities were calculated using LRP assay (Khusro et al., 2018b) against the control (pH 6.5).

#### 2.7.2. Effect of temperature

The effect of temperature on residual anti-tubercular activities was determined using LRP assay (Khusro et al., 2018b). The purified protein (1 mg/mL) at optimum pH level was incubated at 40 °C for 2 h, 60 °C for 1 h, 80 °C 30 min, 100 °C for 20 min, and

121 °C for 15 min. The protein sample without heat treatment was considered as control.

### 2.7.3. Effect of enzymes

Enzymes (1 mg/mL; pepsin – pH 3.0, trypsin – pH 7.5, protease K – pH 7.5, and  $\alpha$ -amylase – pH 7.5) were mixed with purified protein at optimal pH and temperature. The mixture was incubated for 1 h and then subsequently heated at 100 °C for 5 min for inactivating the enzymes. Residual anti-tubercular activities were calculated according to the LRP assay (Khusro et al., 2018b). The purified protein without the addition of enzymes was used as control.

### 2.8. Anticancer activity of purified protein

Anticancer activities of the purified protein (10–50  $\mu$ g/mL) against A549 and HT-29 cancer cells were evaluated using MTT [3-(4,5-dimethylthiazol-2-yl)-2,5-diphenyltetrazolium bromide] assay (Mosmann, 1983). The minimum concentration of protein required for 50% inhibition of cell viability ( $IC_{50}$ ) was calculated using linear regression curve statistics.

### 2.9. Mass spectrometry and N-terminal amino acid sequencing

The protein band of interest (as obtained from SDS-PAGE) was excised from the gel and kept in 50% (v/v) methanol. The protein was digested using trypsin at 37 °C for 12 h. An equal volume of cyano-4-hydrocinnamic acid solution (10 mg/mL CHCA in 70% acetonitrile, 0.03% trifluoro acetic acid) was added to the trypsinized protein. MALDI-TOF MS/MS spectrum determines the fragmentation of protein into various peptides. Peptide mass fingerprinting (PMF) was performed for analyzing the peptide sequences of protein. Mass spectra were recorded in the range of 100–2250  $m/z$ . The N- amino acid sequence was compared with the sequence available in BLAST, NCBI algorithm.

### 2.10. Structure prediction and model evaluation of peptide

The 3D conformation of the identified peptide was predicted using online software PEP-FOLD (<http://bioserv.rpbs.univ-paris-diderot.fr/services/PEP-FOLD3/>) (Beaufays et al., 2012). The quality of peptide structure model was evaluated by determining different stereo-chemical parameters such as Verify 3D, ERRAT, and WHATCHECK using PROCHECK (Laskowski et al., 1993). The stereo-chemical parameters of the peptide were checked by analyzing residue-by-residue and overall structure geometry.

### 2.11. Physicochemical properties of peptide

Physicochemical properties such as amino acids number, theoretical pI (isoelectric point), aliphatic index, instability index, and grand average of hydropathicity (GRAVY) were analyzed using ExPASy–ProtParam tool (<http://web.expasy.org/protparam>) (Dunker and Obradovic, 2001).

### 2.12. Primary structure of peptide

Amino acid composition of the peptide was determined using ExPASy–ProtParam tool (<http://web.expasy.org/protparam>) (Dunker and Obradovic, 2001).

### 2.13. Secondary structure of peptide

Peptide secondary structure was analysed using ExPASy SIB Bioinformatics SOPMA tool which determines number of  $\alpha$ -helices,  $\beta$ -turn, extended strand,  $\beta$ -sheet, and coils. Sequences were

submitted in FASTA format in order to utilize SOPMA. PROCHECK was used for constructing Ramachandran plot (Laskowski et al., 1993).

### 2.14. Functional analysis of peptide

The membrane spanning or extracellular nature of peptide was analyzed using TMHMM tool ([www.cbs.dtu.dk/services/TMHMM](http://www.cbs.dtu.dk/services/TMHMM)).

### 2.15. Statistical analyses

All the experiments were performed in triplicate and results were estimated as mean  $\pm$  SD. Analysis of variance was used for validating the data.  $P \leq 0.05$  were considered statistically significant.

## 3. Results

### 3.1. Anti-tubercular and anticancer activities of strain MANF2

The CFNS of strain MANF2 showed promising activity against *M. tuberculosis* H37Rv, estimating 92.5  $\pm$  1.2% of RLU reduction (Figure not shown). The CFNS of strain showed comparatively higher anticancer activity against A549 cancer cells as compared to HT-29 cells. The viabilities of A549 and HT-29 cancer cell lines were estimated as 76.5  $\pm$  0.4 and 84.2  $\pm$  0.3%, respectively (Figure not shown).

### 3.2. Purification of protein

Protein was purified using standard purification techniques including ammonium sulphate precipitation, dialysis, and DEAE–Cellulose column chromatography. Initially, ammonium sulphate at varied saturation levels (40–80%) was implied to precipitate the protein. Total protein content was estimated based on regression curve equation ( $Y = -0.122 + 0.001 X$ ) obtained (Figure not shown).

Proteins precipitated at 60% saturation showed relatively higher total protein content (1922.3  $\pm$  9.3 mg/L) than that of other saturations (Fig. 1). The protein precipitated with 60% saturation was used for dialysis which revealed total protein content of 188.3 mg with 75.1% recovery and purification fold of 9.58 (Table 1). The dialysed product was further purified using DEAE–Cellulose column chromatography. After column chromatography, the yield and purification fold of protein were estimated to be 69.4% and 507.31, respectively (Table 1). A total of 16 fractions (2 mL) were collected from the elution process and tested for

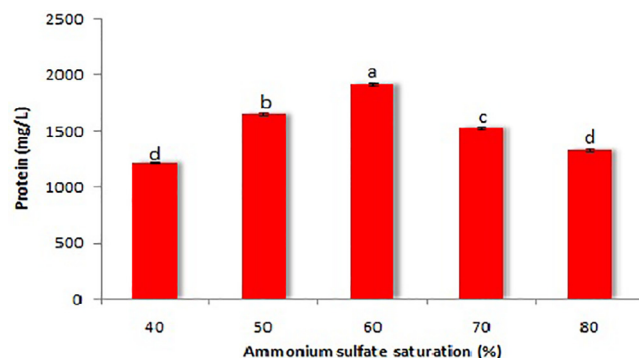


**Fig. 1.** Total protein content determination at different saturation levels of ammonium sulphate. Values are represented as mean  $\pm$  SD of experiments carried out in triplicate ( $n = 3$ ). <sup>abcd</sup>Values with different letters are significantly ( $P < 0.05$ ) different.

**Table 1**  
Purification of protein from strain MANF2.

Purification step	Volume (mL)	RLU (%)	Total protein (mg)	Specific activity	Purification fold	Yield (%)
CFNS	1000	98.7	2432.4	0.041	1	100
Ammonium sulphate precipitation	1000	82.3	1922.3	0.042	1.02	83.4
Dialysis	10	74.1	188.3	0.393	9.58	75.1
DEAE –Cellulose column chromatography	2	68.4	3.3	20.8	507.31	69.4

anti-tubercular activities as well as total protein content determination. Among all the fractions tested, fraction 7 showed maximum protein content and activity. This fraction was lyophilized and used for molecular mass determination. The molecular mass of the purified protein was observed using SDS-PAGE which showed a single homogeneous band corresponding to the molecular mass of approximately 8 kDa based on the relative mobility (Fig. 2).

### 3.3. Fourier transform infra-red spectroscopy

The FT-IR spectrum of the purified protein is shown in Fig. 3. The high absorption bands at 3448.6, 1637.48, 1401.69, and 1085.87  $\text{cm}^{-1}$  indicate the presence of strong N–H stretch, C–N bond of Amide I, N–H bond, and C–N bond, respectively.

### 3.4. Anti-tubercular activity of protein

The anti-tubercular activities of purified protein were increased in a concentration dependent manner (10–50  $\mu\text{g}/\text{mL}$ ) ranging from RLU reduction of  $34.6 \pm 0.3$  to  $71.4 \pm 0.4\%$  with respect to the standard ( $75.5 \pm 0.5$  to  $99.9 \pm 0.5\%$ ) (Fig. 4).

### 3.5. Characterization of protein

The impact of pH, temperature, and enzymes on the residual anti-tubercular activities of purified protein is shown in Table 2. The anti-tubercular activities of protein varied significantly ( $P < 0.05$ ) at various pHs. The protein retained its activity at pH 6.0 and 7.0 with residual activities of  $94.6 \pm 0.5$  and  $96.8 \pm 0.4\%$ . The residual anti-tubercular activities of protein were reduced at

acidic and alkaline pHs. The heat treatment on purified protein exhibited significant ( $P < 0.05$ ) variations in residual activities. The protein retained maximum residual activity of  $96.5 \pm 0.4\%$  at  $40^\circ\text{C}$  for 2 h. The residual anti-tubercular activities were drastically reduced ( $8.6 \pm 0.4\%$ ) at high temperature ( $121^\circ\text{C}$  for 15 min). The anti-tubercular activities of purified protein were lost completely after treatment with pepsin, trypsin, and protease K. On the other hand, the protein was found resistant to  $\alpha$ -amylase, showing residual activity of  $98.2 \pm 0.5\%$ .

### 3.6. Anticancer activity of purified protein

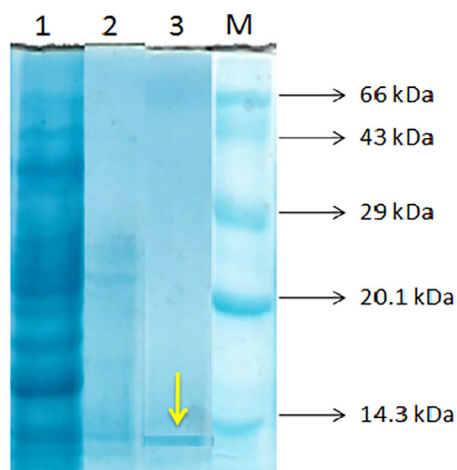
Anticancer activity of the purified protein against A549 cancer cell line is shown in Fig. 5. After treatment with purified protein at various doses, cell shrinkage followed by rounding of cells and reduction in cell counts occurred. The viabilities of A549 cells were reduced ( $96.6 \pm 0.3$ – $46.3 \pm 0.4\%$ ) significantly ( $P < 0.05$ ) with increase in the protein level. A similar morphological alteration was observed in HT-29 cells after treatment with purified protein (Fig. 6). The viabilities of HT-29 cell lines were also reduced ( $98.6 \pm 0.3$ – $49.5 \pm 0.4\%$ ) significantly ( $P < 0.05$ ) with increase in the protein doses. The purified protein revealed comparatively higher anticancer activity against A549 cells with respect to HT-29 cells. The  $\text{IC}_{50}$  values of purified protein against A549 and HT-29 cells were calculated as 46.6 and 48.9  $\mu\text{g}/\text{mL}$ , respectively. In contrary to this, doxorubicin exhibited pronounced anticancer activities with  $\text{IC}_{50}$  values of 7.4 and 9.6  $\mu\text{g}/\text{mL}$  against A549 and HT-29 cells, respectively.

### 3.7. Mass spectrometry and N- terminal amino acid sequencing

Fig. 7 shows MALDI-TOF MS/MS spectrum of purified protein. The nominal mass of purified protein was found to be 7712.3 Da as obtained from PMF analysis. Each peak in the spectrum represents peptides of the purified protein. The size of the peptide ion varies from  $m/z$  101.15 to 1922.12. The most abundant peptide ion is  $m/z$  1922.12. Identification of protein revealed the sequence homology (95%) with 1–336 amino acids of Glyceraldehyde-3-phosphate dehydrogenase from *Staphylococcus* sp. The amino acid sequence of the most abundant peptide ( $m/z = 1922.12$ ) in the purified protein was identified as 'KAIGLVIPEIDGKLDGGAQRV'. Thus, the peptide was identified and named as peptide NMANF2.

### 3.8. Structure prediction and model evaluation of peptide

Fig. 8 shows modelled predicted structure of peptide NMANF2, as determined by PEP-FOLD online tool. Verify 3D, ERRAT, and WHATCHECK were analyzed using PROCHECK server (Table 3). The quality of modelled peptide was analyzed by Verify 3D, and 100% residues of modelled peptide showed a score  $\geq 0.2$ . Therefore, the average 3D–1D scores for all the residues of model were considered 'Pass'. The overall quality factor and compatibility of the model with amino acid residues was evaluated using ERRAT which was calculated as 91.66. In general, the modelled peptide is considered good if the quality factor is  $>50$ . Further, WHATCHECK evaluated the accuracy of modelled peptide structure, thereby indicated that the peptide NMANF2 structure was of reasonably good quality.



**Lane 1:** Ammonium sulphate precipitated sample  
**Lane 2:** Dialysed sample  
**Lane 3:** Purified sample  
**M:** Protein marker

**Fig. 2.** Molecular mass determination of purified protein using SDS-PAGE. Lane 3 showed a single homogeneous band corresponding to the molecular mass of approximately 8 kDa, indicated by yellow arrow.

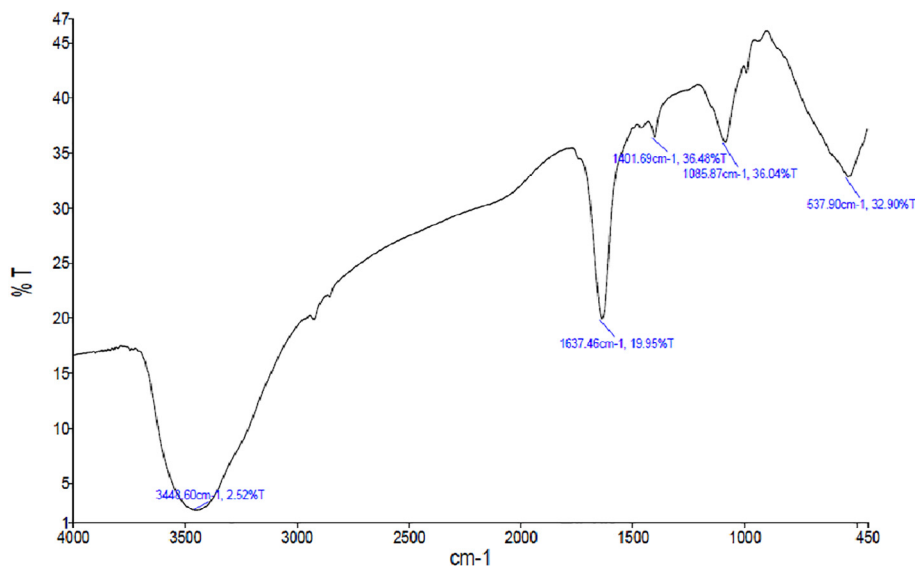


Fig. 3. FT-IR spectrum of purified protein.

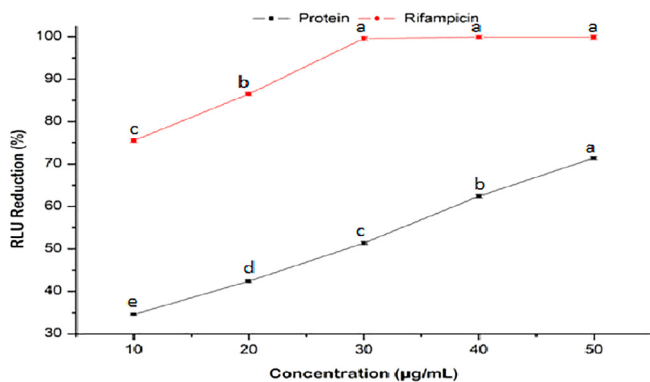


Fig. 4. Anti-tubercular activities of purified protein and rifampicin at various concentrations. Values are represented as mean  $\pm$  SD of experiments carried out in triplicate ( $n = 3$ ). <sup>abcde</sup>Values with different letters are significantly ( $P < 0.05$ ) different.

### 3.9. Physicochemical properties of peptide

Results for physicochemical parameters of peptide NMANF2 are shown in Table 3. The pI of the peptide NMANF2 (Total number of amino acids – 21) was calculated as 6.12. The instability index of the peptide was obtained as 19.3, thereby indicating its stability. Further, the aliphatic index and GRAVY of the peptide were calculated as 130.0 and 0.171, respectively.

### 3.10. Primary structure analysis of peptide

Fig. 9 shows the amino acid composition of peptide NMANF2. The amino acids such as Glycine (19.0%) and Isoleucine (14.3%) were predominant in the peptide. On the other hand, 9.5% of Alanine, Aspartic acid, Leucine, Lysine, and Valine were present in the peptide. While, only 4.8% of Arginine, Glutamine, Glutamic acid, and Proline were available in the peptide.

### 3.11. Secondary structure analysis of peptide

Secondary structure of peptide NMANF2 was dominated by  $\beta$ -turn (42.86%), extended sheet region (33.33%), and random coil (23.81%) (Fig. 10). Fig. 11 shows the percentage of residues in the

Table 2

Effect of pH, temperature, and enzymes on residual anti-tubercular activity of protein.

Treatment	Residual activity (%)
<b>pH</b>	
Control	100 $\pm$ 0.5 <sup>a</sup>
3	41.3 $\pm$ 0.4 <sup>f</sup>
4	48.6 $\pm$ 0.4 <sup>e</sup>
5	53.5 $\pm$ 0.5 <sup>d</sup>
6	94.6 $\pm$ 0.5 <sup>c</sup>
7	96.8 $\pm$ 0.4 <sup>b</sup>
8	52.6 $\pm$ 0.4 <sup>d</sup>
<b>Temperature</b>	
Control	100 $\pm$ 0.5 <sup>a</sup>
40 °C, 2 h	96.5 $\pm$ 0.4 <sup>b</sup>
60 °C, 1 h	51.3 $\pm$ 0.4 <sup>e</sup>
80 °C, 30 min	28.5 $\pm$ 0.5 <sup>d</sup>
100 °C, 20 min	12.3 $\pm$ 0.5 <sup>e</sup>
121 °C, 15 min	8.6 $\pm$ 0.4 <sup>f</sup>
<b>Enzymes</b>	
Control	100 $\pm$ 0.5 <sup>a</sup>
Pepsin	0.00 $\pm$ 0.00
Trypsin	0.00 $\pm$ 0.00
Protease K	0.00 $\pm$ 0.00
$\alpha$ -amylase	98.2 $\pm$ 0.5 <sup>b</sup>

Values represent mean  $\pm$  SD of experiments carried out in triplicate ( $n = 3$ ).

<sup>a,b,c,d,e,f</sup> Means followed by different superscripts are significantly different ( $P < 0.05$ ).

most favourable regions, additionally allowed regions, generously allowed regions, and disallowed regions of Ramachandran plot. About 36% of residues were falling in favoured region, indicating slightly lower stability of this peptide.

### 3.12. Functional analysis of peptide

The membrane spanning or extracellular nature of peptide NMANF2 was analyzed using TMHMM tool which indicated lack of transmembrane domain in the peptide, thereby indicating peptide NMANF2 production extracellularly. Further, the helical wheel prediction of peptide NMANF2 is expressed in Fig. 12 which reveals the availability of hydrophilic and positively charged residues.

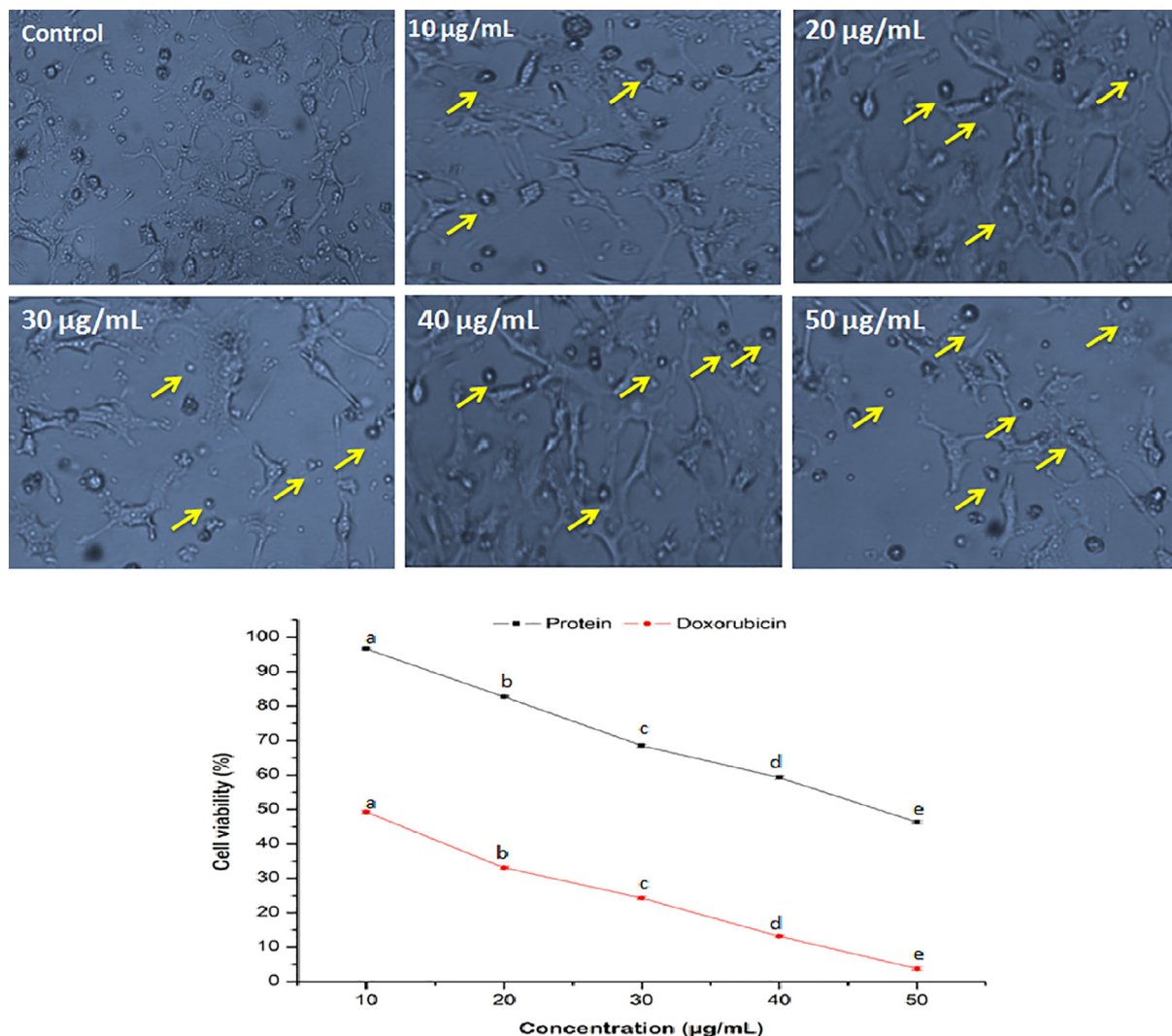


**Fig. 5.** Morphological variations and reduction in the viability of A549 cancer cells in the presence of various concentrations of purified protein. Yellow arrows indicate morphological changes in the cancer cells. Values are represented as mean  $\pm$  SD of experiments carried out in triplicate ( $n = 3$ ). <sup>abcde</sup>Values with different letters are significantly ( $P < 0.05$ ) different.

#### 4. Discussion

Traditional fermented foods associated bacteria are known to produce disparate groups of therapeutic metabolites, particularly enzymes and proteins. These bioactive metabolites contribute not only in the safety but also improve organoleptic properties of foods. In view of the promising antagonistic characteristics of probiotic bacteria against distinct pathogens, its bioactive proteins could be an ideal alternative to the commercially available antibiotics (Aarti et al., 2016, 2017).

Over the past few decades, antibacterial substances, particularly proteins or peptides of bacterial origin have gained tremendous interest as biotherapeutic agents. *Staphylococcus* spp. have been reported to produce a number of bioactive proteinaceous components (Bastos et al., 2009). *S. hominis* MBBL 2–9, *S. pseudintermedius* strain 222, and *S. xylosus* produced novel antibacterial peptide with molecular mass of 6 kDa, 2038.4 Da, and 5921.92 Da, respectively (Kim et al., 2010; Wladyka et al., 2015; Matikevičienė et al., 2017). In this study, strain MANF2 produced anti-tubercular protein of molecular mass 7712.3 Da. Further, based on amino acid sequencing, the molecular mass of the most abundant peptide was obtained as 1922.12 Da, which showed 95% homology with

Glyceraldehyde-3-phosphate dehydrogenase, thereby categorizing it as new class of Glyceraldehyde-3-phosphate dehydrogenase-like protein in *S. hominis*. Also, the peptide was considered new due to the lack of homology of molecular mass with existing peptides previously reported from *Staphylococcus* spp., and thus this peptide was named as NMANF2.

The purified protein exhibited promising anti-tubercular activity in a dose dependent manner, thereby indicating first study on the anti-mycobacterial potentiality of *S. hominis* derived protein. Disparate pH treatment affected significantly the anti-tubercular activity of purified protein. The variation in the anti-tubercular properties at lower or higher pH may be due to the denaturation of protein as electrostatic repulsion of intermolecular and breaking of hydrogen bonds (Yi et al., 2016). Further, the protein lost its anti-tubercular activity at high temperature ( $>60$  °C). It clearly suggests that heat resistance nature of protein depends on its stable structural characteristics (Kim et al., 2010). The anti-tubercular traits of purified protein were lost completely after treatment with pepsin, trypsin, and protease K but its mycobactericidal attribute was retained by  $\alpha$ -amylase treatment. The findings clearly represent that the purified product is proteinaceous in nature constituting amino acid residues, without carbohydrate moieties. Similar

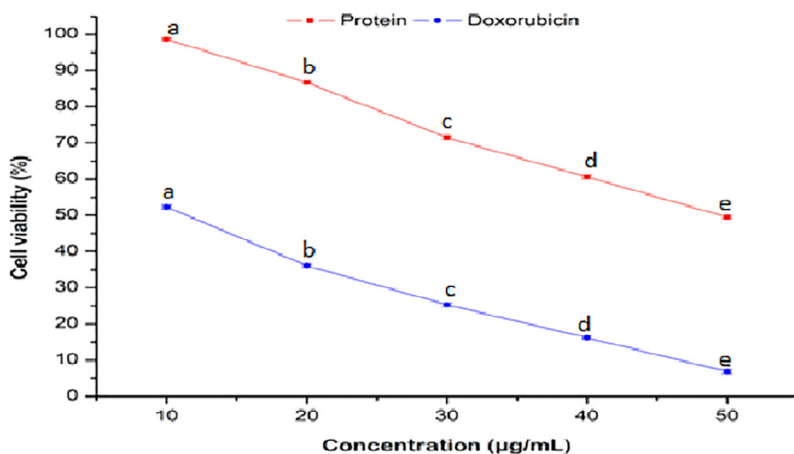
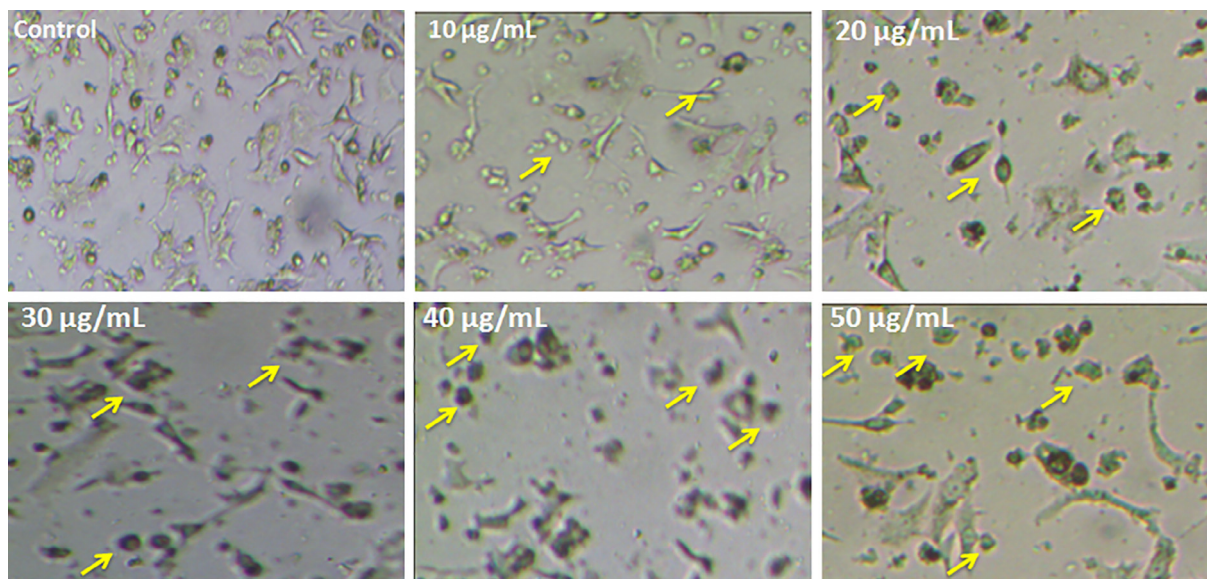


**Fig. 6.** Morphological variations and reduction in the viability of HT-29 cancer cells in the presence of various concentrations of purified protein. Yellow arrows indicate morphological changes in the cancer cells. Values are represented as mean  $\pm$  SD of experiments carried out in triplicate ( $n = 3$ ). <sup>abcde</sup>Values with different letters are significantly ( $P < 0.05$ ) different.

observations were reported by previous studies too (Kim et al., 2010; Yi et al., 2016).

In the present investigation, the *in vitro* cytotoxic activities of purified protein were determined against lung and colon cancer cells. The protein revealed comparatively higher anticancer activity against A549 cells with respect to HT-29 cells. Findings of this context indicated the first investigation in terms of revealing anticancer attribute of *S. hominis* associated protein. The purified protein can undeniably be used for designing new protein-based anticancer drug against lung and colon cancer.

FT-IR spectroscopy is a powerful tool to provide information about the conformational and structural dynamics of a metabolite (Esther Lydia et al., 2019). In this study, the FT-IR spectrum of the purified protein indicated strong peaks, suggesting the presence of varied functional groups. Various peaks in the protein represent stretching and bending vibrations in infrared radiation region.

Stereo-chemical parameters are used to assess the quality of protein or peptide structures generated through various tools. Verify 3D is one of the most important stereo-chemical parameters which is implemented to evaluate the residue profile of the 3D model of specific protein or peptide studied (Luthy et al., 1992). In this study, Verify 3D showed 100% compatibility for the 3D

model of peptide NMANF2. ERRAT is a structure evaluation server which predicts the quality assessment of stable models of proteins or peptides. In this study, ERRAT value of peptide NMANF2 is within the acceptable range. According to the report of Singh et al. (2016), any modelled structure exhibiting ERRAT score value of more than 50 is considered good. Likewise, WHATCHECK is another pivotal stereo-chemical parameter which is also used to assess the accuracy of modelled structure. WHATCHECK indicates that the structure of peptide NMANF2 is of reasonably good quality. Similar observation was reported by Singh et al. (2016) too.

Physicochemical parameters are the preliminary properties of proteins or peptides which depicts their uniqueness. Isoelectric point (pI) is the pH at which the surface of protein is charged but net charge of protein is zero (Dutta et al., 2018). The nature of the macromolecule is alkaline if the theoretical pI value is more than 7. The theoretical pI  $< 7$  indicates the acidity of the molecule. In this context, theoretical pI of peptide NMANF2 was determined acidic in nature. Instability index is another crucial parameter which evaluates the uniqueness of the protein or peptide. Instability index value of any protein below 40 is considered stable (Dutta et al., 2018). In our study, the instability index value of peptide NMANF2 was calculated as 19.3, thereby indicating stability of this

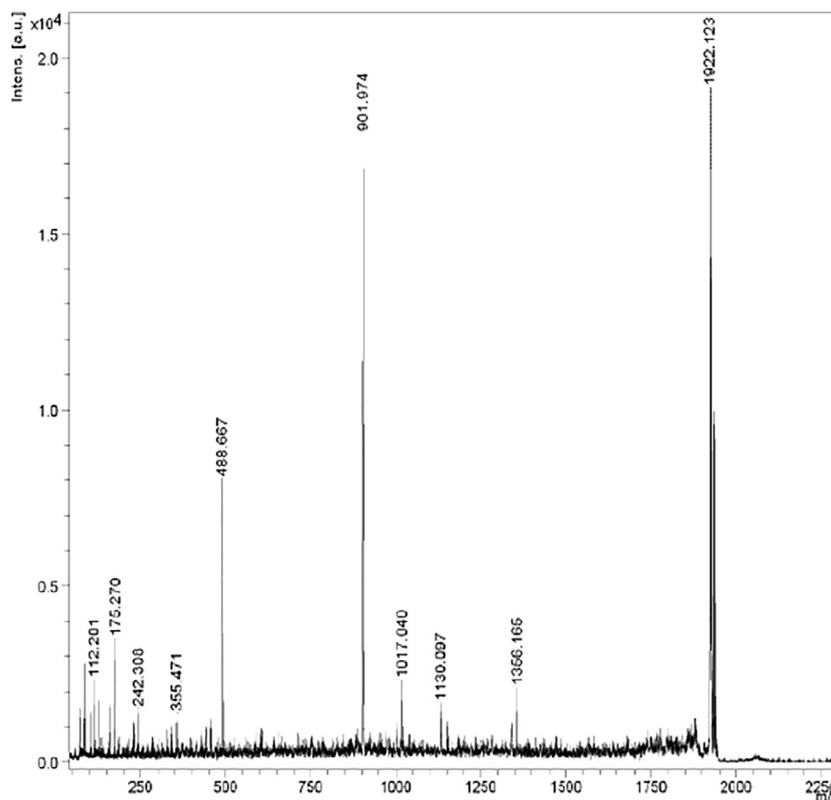


Fig. 7. MALDI-TOF MS/MS spectrum of purified protein.

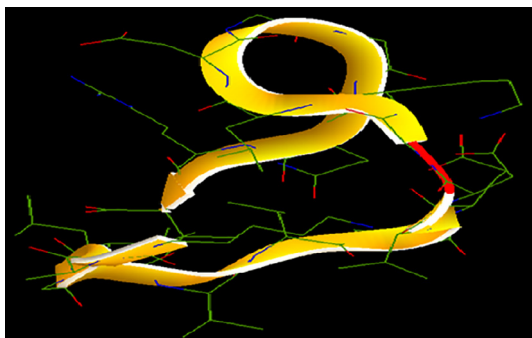


Fig. 8. Structure of peptide NMANF2.

peptide. The relative volume of peptide occupied by aliphatic amino acids in the side chain is determined by its aliphatic index value. A high aliphatic index value more than 50 represents that the particular protein is temperature stable. In general, the aliphatic index is directly proportional to the thermo-stability of the protein or peptide (Dutta et al., 2018). In this study, peptide NMANF2 exhibited the aliphatic index value of 130.0, which indicates its stability towards high temperature. Hydropathicity represents the relative hydrophobicity or hydrophilicity of amino acids

(Kusumaningtyas et al., 2016). In this study, the GRAVY value of peptide NMANF2 represents its potential interaction with water.

Primary structure of peptides depicts the composition of amino acid. In this context, Glycine (19.0%) and Isoleucine (14.3%) were predominant in the peptide NMANF2. On the other hand, Alanine, Aspartic acid, Leucine, Lysine, Valine, Arginine, Glutamine, Glutamic acid, and Proline were present in comparatively lower amount. In general, the predominance of Glycine provides high flexibility to the protein or peptide (Dutta et al., 2018; Balachandran et al., 2015).

Secondary structure of peptide NMANF2 was dominated by  $\beta$ -turn (42.86%), extended sheet region (33.33%), and random coil (23.81%). Thus, the finding illustrates that the peptide has slightly lower structure stability as it is mainly composed of  $\beta$ -turn. Ramachandran angles determine the rotation of the polypeptide backbone around the bonds between N-C $_{\alpha}$  ( $\Phi$ ) and C $_{\alpha}$ -C ( $\Psi$ ) (Singh et al., 2016). Ramachandran plot shows the percentage of residues in favourable regions, additionally allowed regions, generously allowed regions, and disallowed regions. In this study, about 36% of residues were falling in favoured region, indicating slightly lower stability of this peptide. The membrane spanning or extracellular nature of the peptide was analyzed using TMHMM tool which indicated extracellular production of peptide NMANF2. Further, the helical wheel prediction of peptide NMANF2 showed the presence of hydrophilic and positively charged residues, thus, supporting the findings of Xin et al. (2017).

**Table 3**  
Stereo-chemical and physiochemical parameters of peptide.

Peptide	Stereo-chemical and physiochemical parameters							
	Verify 3D	ERRAT	WHATCHECK	Number of amino acids	Theoretical pI	Instability index	Aliphatic index	GRAVY
NMANF2	100%	91.66	Good	21	6.12	19.3	130.0	0.171

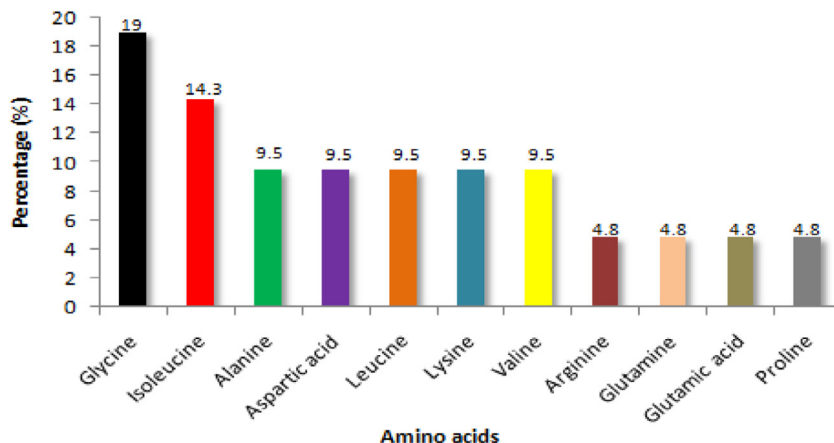


Fig. 9. Amino acid composition (%) of peptide NMANF2.

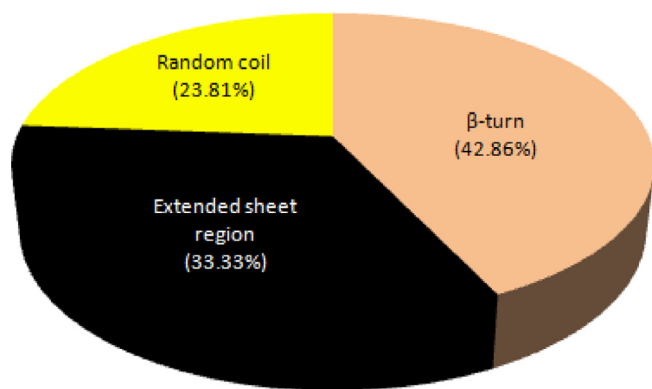


Fig. 10. Secondary structure of peptide NMANF2 was dominated by β-turn, extended sheet region, and random coil.

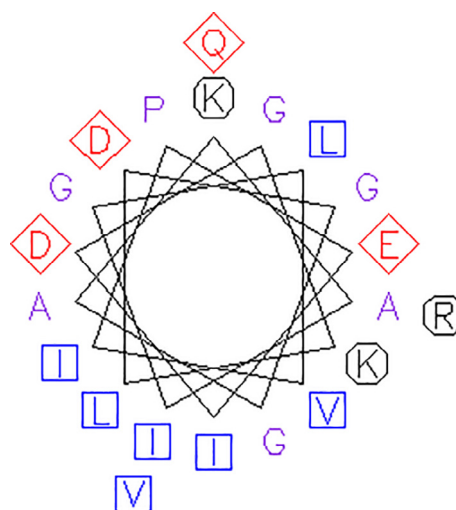


Fig. 12. The helical wheel prediction of peptide NMANF2. Aliphatic residues are marked with squares, hydrophilic residues are marked with diamonds, and positively charged residues with octagons.

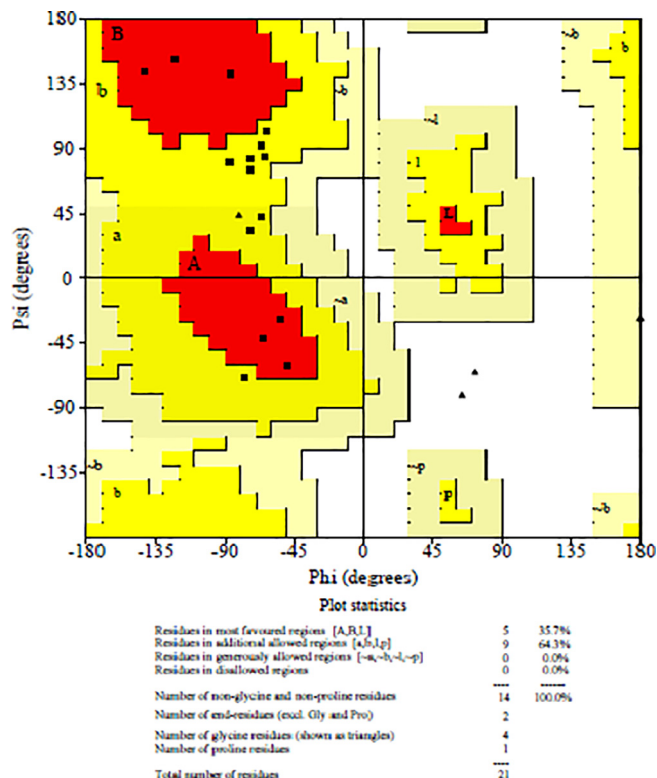


Fig. 11. Ramachandran plot showing percentage of residues in the most favourable regions, additionally allowed regions, generously allowed regions, and disallowed regions.

5. Conclusions

The study represents the first study on the purification of anti-tubercular and anticancer protein from *S. hominis*. The nominal mass of the purified protein was obtained as 7712.3 Da, revealing sequence homology (95%) with Glyceraldehyde-3-phosphate dehydrogenase from *Staphylococcus* sp. It is a new Glyceraldehyde-3-phosphate dehydrogenase-like protein. The molecular mass of the most abundant peptide was observed as 1922.12 Da, and thus, the peptide was named as NMANF2. *In silico* investigations clearly indicated the promising stereo-chemical, physiochemical, and functional characteristics of peptide NMANF2. Strain MANF2 associated protein can be utilized as an ideal therapeutic agent against TB and cancer (lung and colon).

Declaration of Competing Interest

Authors declare that they have no known competing financial interests or personal relationships that could have appeared to influence the work reported in this paper.

Acknowledgement

Authors acknowledge Maulana Azad National Fellowship (F1-17.1/2015-16/MANF-2015-17-BIH-60730), University Grants

Commission, Delhi, India for the support. Also, authors would like to extend their sincere appreciation to the Deanship of Scientific Research at King Saud University for its funding of this research through the Research Group Project No. RG-1440-107.

## References

- Aarti, C., Khusro, A., Arasu, M.V., Agastian, P., Al-Dhabi, N.A., 2016. Biological potency and characterization of antibacterial substances produced by *Lactobacillus pentosus* isolated from *Hentak*, a fermented fish product of North-East India. *SpringerPlus* 5, 1743. <https://doi.org/10.1186/s40064-016-3452-2>.
- Aarti, C., Khusro, A., Varghese, R., Arasu, M.V., Agastian, P., Al-Dhabi, N.A., et al., 2017. *In vitro* studies on probiotic and antioxidant properties of *Lactobacillus brevis* strain LAP2 isolated from *Hentak*, a fermented fish product of North-east India. *LWT Food Sci. Technol.* 86, 438–446.
- Al-Dhabi, N.A., Esmail, G.A., Duraipandiyani, V., Valan, Arasu M., 2019a. Chemical profiling of *Streptomyces* sp. Al-Dhabi-2 recovered from an extreme environment in Saudi Arabia as a novel drug source for medical and industrial applications. *Saudi J. Biol. Sci.* 26, 758–766.
- Al-Dhabi, N.A., Esmail, G.A., Duraipandiyani, V., Valan Arasu, M., Salem-Bekhit, M.M., 2016. Isolation, identification and screening of antimicrobial thermophilic *Streptomyces* sp. Al-Dhabi-1 isolated from Tharban hot spring Saudi Arabia. *Extremophiles* 20, 79–90.
- Al-Dhabi, N.A., Esmail, G.A., Ghilan, A.-K.M., Arasu, M.V., 2020. Isolation and screening of *Streptomyces* sp. Al-Dhabi-49 from the environment of Saudi Arabia with concomitant production of lipase and protease in submerged fermentation. *Saudi J. Biol. Sci.*, 474–479 <https://doi.org/10.1016/j.sjbs.2019.11.011>.
- Al-Dhabi, N.A., Esmail, G.A., Ghilan, A.-K.M., Arasu, M.V., Duraipandiyani, V., Ponnurugan, K., 2019b. C Isolation and purification of starch hydrolysing amylase from *Streptomyces* sp. Al-Dhabi-46 obtained from the Jazan region of Saudi Arabia with industrial applications. *J. King Saud Univ.-Sci.* <https://doi.org/10.1016/j.jksus.2019.11.018>.
- Al-Dhabi, N.A., Esmail, G.A., Ghilan, A.-K.M., Arasu, M.V., Duraipandiyani, V., Ponnurugan, K., 2019c. Characterization and fermentation optimization of novel thermo stable alkaline protease from *Streptomyces* sp. Al-Dhabi-82 from the Saudi Arabian environment for eco-friendly and industrial applications. *J. King Saud Univ.-Sci.* <https://doi.org/10.1016/j.jksus.2019.11.011>.
- Al-Dhabi, N.A., Esmail, G.A., Ghilan, A.K.M., Arasu, M.V., Duraipandiyani, V., Ponnurugan, K., 2019e. Chemical constituents of *Streptomyces* sp. strain AlDhabi-97 isolated from the marine region of Saudi Arabia with antibacterial and anticancer properties. *J. Infect Public Health.* <https://doi.org/10.1016/j.jiph.2019.09.004>.
- Al-Dhabi, N.A., Ghilan, A.K.M., Arasu, M.V., Duraipandiyani, V., 2019f. Green biosynthesis of silver nanoparticles produced from marine *Streptomyces* sp. Al-Dhabi-89 and their potential applications against wound infection and drug resistant clinical pathogens. *J. Photochem. Photobiol. B*, 111529.
- Al-Dhabi, N.A., Ghilan, A.K.M., Arasu, M.V., Duraipandiyani, V., Ponnurugan, K., 2018a. Environmental friendly synthesis of silver nanomaterials from the promising *Streptomyces parvus* strain Al-Dhabi-91 recovered from the Saudi Arabian marine regions for antimicrobial and antioxidant properties. *J. Photochem. Photobiol. B* 189, 176–184.
- Al-Dhabi, N.A., Mohammed Ghilan, A.K., Esmail, G.A., Valan Arasu, M., Duraipandiyani, V., Ponnurugan, K., 2019g. Bioactivity assessment of the Saudi Arabian Marine *Streptomyces* sp. Al-Dhabi-90, metabolic profiling and its *in vitro* inhibitory property against multidrug resistant and extended-spectrum betalactamase clinical bacterial pathogens. *J. Infect. Public Health* 12, 549–556.
- Arasu, M.V., Duraipandiyani, V., Ignacimuthu, S., 2013. Antibacterial and antifungal activities of polyketide metabolite from marine *Streptomyces* sp. AP-123 and its cytotoxic effect. *Chemosphere* 90 (2), 479–487.
- Arasu, M.V., Thirumamagal, R., Srinivasan, M.P., Al-Dhabi, N.A., Ayeshamariam, A., Saravana Kumar, D., Punithavel, N., Jayachandran, M., 2017. Green chemical approach towards the synthesis of CeO<sub>2</sub> doped with seashell and its bacterial applications intermediated with fruit extracts. *J. Photochem. Photobiol. B* 172, 50–60.
- Balachandran, C., Duraipandiyani, V., Emi, N., Ignacimuthu, S., 2015. Antimicrobial and cytotoxic properties of *Streptomyces* sp. (ERINLG-51) isolated from Southern/Western Ghats. *South Indian J. Biol. Sci.* 1, 7–14.
- Bastos, M.C.F., Ceotto, H., Coelho, M.L.V., Nascimento, J.S., 2009. Staphylococcal antimicrobial peptides: Relevant properties and potential biotechnological applications. *Curr. Pharm. Biotechnol.* 10, 38–61.
- Beaufays, J., Lins, L., Thomas, A., Brasseur, R., 2012. *In silico* predictions of 3D structures of linear and cyclic peptides with natural and non-proteinogenic residues. *J. Pept. Sci.* 18, 17–24.
- Bradford, M.M., 1976. A rapid and sensitive method for the quantitation of microgram quantities, of protein utilizing the principle of protein-dye binding. *Anal. Biochem.* 72, 248–254.
- De-Oliveira, S.S., Abrantes, J., Cardoso, M., Sordelli, D., Bastos, M.C., 1998. Staphylococcal strains involved in bovine mastitis are inhibited by *Staphylococcal aureus* antimicrobial peptides. *Lett. Appl. Microbiol.* 27, 287–291.
- Dunker, A.K., Obradovic, Z., 2001. The protein trinity—linking function and disorder. *Nat. Biotechnol.* 19, 805–806. <https://doi.org/10.1038/nbt0901-805>.
- Dutta, B., Banerjee, A., Chakraborty, P., Bandopadhyay, R., 2018. *In silico* studies on bacterial xylanase enzyme: Structural and functional insight. *J. Genet. Eng. Biotechnol.* 16, 749–756.
- Esther Lydia, D., Gupta, C., Khusro, A., Salem, A.Z.M., 2019. Susceptibility of poultry associated bacterial pathogens to *Momordica charantia* fruits and evaluation of *in vitro* biological properties. *Microb. Pathogen.* 132, 222–229.
- Hale, E.M., Hinsdill, R.D., 1973. Characterization of a bacteriocin from *Staphylococcus aureus* strain 462. *Antimicrob. Agents Chemother.* 4, 634–640.
- Iqbal, A., Ali, S.A., Abbasi, A., Volter, W., Rasool, S.A., 2001. Production and some properties of Bac201: a bacteriocin like inhibitory substance from *Staphylococcus aureus* AB201. *J. Basic Microbiol.* 41, 25–36.
- Kaur, S., Kaur, S., 2015. Bacteriocins as potential anticancer agents. *Front. Pharmacol.* 6, 272. <https://doi.org/10.3389/fphar.2015.00272>.
- Khusro, A., Aarti, C., Agastian, P., 2016. Anti-tubercular peptides: A quest of future therapeutic weapon to combat tuberculosis. *Asian Pac. J. Trop. Med.* 9, 1023–1034.
- Khusro, A., Aarti, C., Dusthacker, A., Agastian, P., 2018a. Enhancement of anti-tubercular activity and biomass of fermented food associated *Staphylococcus hominis* strain MANF2 using Taguchi orthogonal array and Box-Behnken design. *Microb. Pathogen.* 120, 8–18.
- Khusro, A., Aarti, C., Dusthacker, A., Agastian, P., 2018b. Anti-tubercular and probiotic properties of coagulase-negative staphylococci isolated from *Koozh*, a traditional fermented food of South India. *Microb. Pathogen.* 114, 239–250.
- Kim, P., Sohng, J.K., Sung, C., Joo, H.S., Kim, E.M., Yamaguchi, T., et al., 2010. Characterization and structure identification of an antimicrobial peptide, homininin, produced by *Staphylococcus hominis* MBBL 2–9. *Biochem. Biophys. Res. Commun.* 399, 133–138.
- Kusumaningtyas, E., Widiastuti, R., Kusumaningrum, H.D., Suhartono, M.T., 2016. Sequence analysis and modeling of antimicrobial peptide from goat milk protein hydrolyzed by bromelain. *Proc. Intsem. LPVT-2016*, 327–335.
- Laskowski, R.A., MacArthur, M.W., Moss, D.S., Thornton, J.M., 1993. PROCHECK - a program to check the stereochemical quality of protein structures. *J. App. Cryst.* 26, 283–291.
- Luthy, R., Bowie, J.U., Eisenberg, D., 1992. Assessment of protein models with three-dimensional profiles. *Nature* 356, 83–85.
- Matikevičienė, V., Grigiškis, S., Lubytė, E., Dienys, G., 2017. Partial purification and characterization of bacteriocin-like peptide produced by *Staphylococcus xylosum*. *Environ. Technol. Resour.* 3, 213–216.
- Mosmann, T., 1983. Rapid colorimetric assay for cellular growth and survival: application to proliferation and cytotoxicity assays. *J. Immunol. Methods* 65, 55–63.
- Nascimento, J.S., Fagundes, P.C., de Paiva Brito, M.A.V., dos Santos, K.R.N., de Freire Bastos, M.C., 2005. Production of bacteriocins by coagulase-negative staphylococci involved in bovine mastitis. *Vet. Microbiol.* 106, 61–71.
- Navartana, M.A., Sahl, H.G., Tagg, J.R., 1998. Two component anti-*Staphylococcus aureus* lantibiotic activity produced by *Staphylococcus aureus* C55. *Appl. Environ. Microbiol.* 64, 4803–4808.
- Saeed, S., Ahmad, S., Rasool, S.A., 2004. Antimicrobial spectrum, production and mode of action of staphylococin 188 produced by *Staphylococcus aureus* 188. *Pakistan J. Pharm. Sci.* 17, 1–8.
- Singh, S., Singh, D.B., Singh, A., Ram, B.G.G., Dwivedi, S., Ramteke, P.W., 2016. An approach for identification of novel drug targets in *Streptococcus pyogenes* SF370 through pathway analysis. *Interdiscip. Sci. Comput. Life Sci.* 8, 388–394.
- Sung, C., Kim, B.G., Kim, S., Joo, H.S., Kim, P.I., 2010. Probiotic potential of *Staphylococcus hominis* MBBL 2–9 as anti-*Staphylococcus aureus* agent isolated from the vaginal microbiota of a healthy woman. *J. Appl. Microbiol.* 108, 908–916.
- Wladyka, B., Piejko, M., Bzowska, M., Pieta, P., Krzysik, M., Mazurek, L., et al., 2015. A peptide factor secreted by *Staphylococcus pseudintermedius* exhibits properties of both bacteriocins and virulence factors. *Sci. Rep.* 5, 14569.
- Al-Dhabi, N.A., Esmail, G.A., Ghilan, A.-K.M., Arasu, M.V., Duraipandiyani, 2019e. Metabolite profiling of *Streptomyces* sp. Al-Dhabi-100 isolated from the marine environment in Saudi Arabia with anti-bacterial, anti-tubercular and antioxidant potentials. *J. King Saud Univ.-Sci.* doi: 10.1016/j.jksus.2019.12.021.
- Al-Dhabi, N.A., Ghilan, A.-K.M., Arasu, M.V., 2018b. Characterization of silver nanomaterials derived from marine *Streptomyces* sp. Al-Dhabi-87 and its *in vitro* application against multidrug resistant and extended-spectrum betalactamase Clinical Pathogens. *Nanomater.* 8 (5).
- World Cancer Report 2014. World Health Organization. 2014. pp. Chapter 5.1. ISBN 92-832-0429-8
- Xin, H., Ji, S., Peng, J., Han, P., An, X., Shan Wang, et al., 2017. Isolation and characterisation of a novel antibacterial peptide from a native swine intestinal tract-derived bacterium. *Int. J. Antimicrob. Agents* 49, 427–436.
- Yi, L., Dang, Y., Wu, J., Zhang, L., Liu, X., Liu, B., et al., 2016. Purification and characterization of a novel bacteriocin produced by *Lactobacillus crustorum* MNO47 isolated from koumiss from Xinjiang, China. *J. Dairy Sci.* 99, 7002–7015.